



Ingenius. Revista de Ciencia y Tecnología  
ISSN: 1390-650X  
ISSN: 1390-860X  
revistaingenius@ups.edu.ec  
Universidad Politécnica Salesiana  
Ecuador

## ON THE BEHAVIOUR OF SPHERICAL INCLUSIONS IN A CYLINDER UNDER TENSION LOADS

---

**Montero, Sebastián; Bustamante., Roger; Ortiz-Bernardin, Alejandro**

ON THE BEHAVIOUR OF SPHERICAL INCLUSIONS IN A CYLINDER UNDER TENSION LOADS

Ingenius. Revista de Ciencia y Tecnología, no. 19, 2018

Universidad Politécnica Salesiana, Ecuador

**Available in:** <https://www.redalyc.org/articulo.oa?id=505554803007>

**DOI:** <https://doi.org/10.17163/ings.n19.2018.07>




This work is licensed under Creative Commons Attribution-NonCommercial-ShareAlike 3.0 International.

ON THE BEHAVIOUR OF SPHERICAL INCLUSIONS IN A CYLINDER UNDER TENSION LOADS

ESTUDIO DEL COMPORTAMIENTO DE INCLUSIONES ESFÉRICAS EN UN CILINDRO BAJO TRACCIÓN

*Sebastián Montero*

*University of Chile, Chile*

 <http://orcid.org/0000-0002-2402-6139>

DOI: <https://doi.org/10.17163/ings.n19.2018.07>

Redalyc: <https://www.redalyc.org/articulo.oa?id=505554803007>

*Roger Bustamante.*

*University of Chile, Ecuador*

[rogbusta@ing.uchile.cl](mailto:rogbusta@ing.uchile.cl)

 <http://orcid.org/0000-0002-1072-1042>

*Alejandro Ortiz-Bernardin*

*University of Chile, Chile*

 <http://orcid.org/0000-0001-9221-2470>

Received: 10 October 2017

Accepted: 19 December 2017

## ABSTRACT:

In the present paper the behaviour of a hyperelastic body is studied, considering the presence of one, two and more spherical inclusions, under the effect of an external tension load. The inclusions are modeled as nonlinear elastic bodies that undergo small strains. For the material constitutive relation, a relatively new type of model is used, wherein the strains (linearized strain) are assumed to be nonlinear functions of the stresses. In particular, it is used a function such that the strains are always small, independently of the magnitude of the external loads. In order to simplify the problem, the hyperelastic medium and the inclusions are modelled as axial-symmetric bodies. The finite element method is used to obtain results for these boundary value problems. The objective of using these new models for elastic bodies in the case of the inclusions is to study the behaviour of such bodies in the case of concentration of stresses, which happens near the interface with the surrounding matrix. From the results presented in this paper, it is possible to observe that despite the relatively large magnitude for the stresses, the strains for the inclusions remain small, which would be closer to the actual behaviour of real inclusions made of brittle materials, which cannot show large strains.

**KEYWORDS:** Energy Saving, Characterization, Goal, Production.

## RESUMEN:

En el presente artículo se estudia el comportamiento de un sólido hiper-elástico con una, dos y más inclusiones esféricas, bajo el efecto de una carga externa de tracción. Las inclusiones se modelan como sólidos elásticos con comportamiento no-lineal y que presentan pequeñas deformaciones, usando un nuevo modelo propuesto recientemente en la literatura, en donde las deformaciones (caso infinitesimal) se expresan como funciones no-lineales de las tensiones. En particular, se consideran expresiones para dichas funciones que aseguran que las deformaciones están limitadas en cuanto a su magnitud independientemente de la magnitud de las cargas externas. Como una forma de simplificar el problema, el medio hiper-elástico y las inclusiones se modelan como sólidos axil-simétricos. El método de elementos finitos es usado para obtener resultados para estos problemas de valor de frontera. El objetivo del uso de los nuevos modelos para cuerpos elásticos para el caso de las inclusiones, es estudiar el comportamiento de dichos cuerpos en el caso de concentración de tensiones, lo cual ocurre cerca de la zona de interface con la matriz. De los resultados mostrados en este trabajo, es posible apreciar que a pesar de los valores relativamente altos para las tensiones, las deformaciones se mantienen pequeñas, lo cual sería mucho más cercano al comportamiento esperado en la realidad, cuando se trabaja con inclusiones hechas de un material frágil, el cual no puede mostrar grandes deformaciones.

**PALABRAS CLAVE:** ahorro de energía, caracterización, meta, producción.

## FORMA SUGERIDA DE CITACIÓN:

Montero, S.; Bustamante, R.; Ortiz-Bernardin, A. (2018). «On the behaviour of spherical inclusions in a cylinder under tension loads». Ingenius. N.º 19, (january-june). pp. 69-78. doi: <https://doi.org/10.17163/ings.n19.2018.07>.

## 1. INTRODUCTION

In Refs. [1–3] Rajagopal and co-workers have proposed some new types of constitutive relations, which cannot be classified as either Green or Cauchy elastic equations. If  $T$  and  $B$  are used to denote the Cauchy stress tensor and the left Cauchy Green tensor, respectively, one of such relations is  $f(T, B) = 0$ , and two special cases that can be obtained from the above implicit relation are the classical nonlinear constitutive equation for a Cauchy elastic body [4]  $T = g(B)$ , and the subclass  $B = h(T)$  (see, for example, Ref. [5]).

As a particular case, we assume that the gradient of the displacement field is small. From the above equation  $B = h(T)$ , we obtain  $\varepsilon = g(T)$ , where  $\varepsilon$  is the linearized strain tensor. This last constitutive equation is very important on its own, since it could be used to model the behavior of some materials that can show a nonlinear behavior, but where the strains are small, such as rock [6, 7], concrete [8] and some metal alloys [9]. Another important use of  $\varepsilon = g(T)$  is in the fracture mechanics analysis of brittle bodies [10], where for some particular expressions for  $g(T)$ , it can be proved that for a crack in a brittle body, the magnitude of the strains are limited and do not go to infinite near the tip of a crack, contrary to what happens when the classical linearized elastic theory is used (see, for example, Ref. [11]). It is very important to study the behaviour of elastic bodies considering  $\varepsilon = g(T)$  for as many different boundary value problems as possible, in order to understand the capabilities and drawbacks of these new constitutive models, and that is the main objective of the present communication.

We are interested in studying the behaviour of a hyper-elastic (Green solid) cylindrical sample that can contain 1, 2 and 5 spherical inclusions, which are located in a row in the central axis of the cylinder, and which are equally separated from each other. The inclusions are assumed to behave as nonlinear elastic solids, using the new constitutive equation  $\varepsilon = g(T)$  mentioned above. For simplicity the composite sample is modeled as an axial-symmetric body and a tension load is applied on the upper part of the cylinder. The finite element method is used to obtain results for the boundary value problem. We are particularly interested in studying the behaviour of the stresses and strains near the interface of the inclusions and the surrounding hyper-elastic body. It is assumed that the spherical inclusions are perfectly attached to the hyper-elastic matrix. The hypothesis of our work is that the new classes of constitutive equations  $\varepsilon = g(T)$  can be useful for the modelling of brittle bodies, in particular in the case we have large stresses, but where the strains must remain small. For a cylindrical sample with inclusions, such concentration of stresses appear near the interface of the matrix and the inclusion, and as it is shown in the present work, considering a particular expression for  $g(T)$ , that we indeed obtain small strains for the spherical inclusions. For the modelling of such composite materials is very important to obtain results as precise as possible of the stresses near the interface, as the most common failure, which such composites show, corresponds to the debonding of the particles with the surrounding matrix.

This work is structured into the following sections. In Section 2 we present the basic equations for the models, in particular, the constitutive equations used for the spherical inclusions. In Section 3 we give details about the models to be analyzed. In Section 4, some numerical results for the different cases analyzed are presented. We end in Section 5 with some concluding remarks about the numerical results presented in this paper.

## 2. BASIC EQUATIONS

### 2.1. Kinematics and equation of motion

Let  $X$  denotes a point of a body  $B$ , the reference and current configurations are denoted as  $B_r$  and  $B_t$ , respectively, and the position of point  $X$  in such configurations is denoted as  $X$  and  $x$ , respectively. It is assumed that there is a one-to-one mapping such that  $x = (X, t)$ , where  $t$  is time. The deformation gradient  $F$ , the left and the right Cauchy-Green tensors  $B$ ,  $C$ , respectively, the Green Saint-Venant strain tensor  $E$ , the displacement field  $u$  and the linearized strain tensor  $\epsilon$  are defined as:

$$F = \frac{\partial x}{\partial X}, \quad B = FF^T, \quad C = F^T F, \quad (1)$$

$$E = \frac{1}{2}(C - I), \quad u = x - X, \quad (2)$$

$$\epsilon = \frac{1}{2}(\nabla u + \nabla u^T), \quad (3)$$

Respectively, where  $\Delta$  is the gradient operator with respect to the reference configuration. We assume  $0 < J < \infty$ , where  $J = \det F$ .

The equation of motion is

$$\rho \ddot{x} = \operatorname{div} T + \rho b, \quad (4)$$

where  $\rho$  is the density of the body in the current configuration,  $T$  is the Cauchy stress tensor,  $b$  represents the body forces in the current configuration,  $(\ddot{\phantom{x}})$  is the second derivative in time, and  $\operatorname{div}$  is the divergence operator defined in the current configuration.

In our work we consider quasi-static deformations, therefore the left side of (4) is zero. More details about the above relations can be found, for example, in Ref. [13].

### 2.2. Constitutive equations

We consider a body composed of two materials, a matrix which is assumed to be hyper-elastic, filled with spherical inclusions which are assumed to behave as nonlinear elastic bodies undergoing small strains. For the hyper-elastic matrix cylinder, we assume there exists a function  $W = W(F)$ , called the energy function, such that (see, for example, Ref. [4])

$$T = J^{-1} F \frac{\partial W}{\partial F}, \quad (5)$$

where we use the convention  $(\frac{\partial W}{\partial F})_{\alpha i} = \frac{\partial W}{\partial F_{\alpha i}}$ . In this work, we use the neo-Hookean compressible model

$$W = \frac{\mu}{2}(\bar{I}_1 - 3) + \frac{\kappa}{2}(J - 1)^2, \quad (6)$$

Where  $\bar{I}_1 = J^{-1/3}I_1$ ,  $I_1 = \text{tr}(\mathbf{C})$ , where  $\text{tr}$  is the trace of a second order tensor, and  $\mu, \kappa$  are material constants.

For the inclusions, we assume that they are elastic bodies that develop nonlinear behavior when strains are small. As indicated in the introduction section, recently some new types of constitutive relations for elastic bodies have been proposed in the literature [1–3], one of such relations is of the form

$$\mathbf{f}(\mathbf{T}, \mathbf{B}) = \mathbf{0}, \quad (7)$$

where the Cauchy elastic body  $\mathbf{T} = \mathbf{g}(\mathbf{B})$  is a special subclass of the above relation, plus the new constitutive equation

$$\mathbf{B} = \mathbf{h}(\mathbf{T}). \quad (8)$$

Assuming that  $|\nabla \mathbf{u}| \sim O(\delta)$  where  $\delta \ll 1$ , then  $\mathbf{B} \approx 2\boldsymbol{\varepsilon} + \mathbf{I}$  (we also have  $\mathbf{E} \approx \boldsymbol{\varepsilon}$ ), and from (8) we obtain (see, for example, Refs. [14, 15])

$$\boldsymbol{\varepsilon} = \mathbf{g}(\mathbf{T}), \quad (9)$$

where in general  $\mathbf{g}(\mathbf{T})$  is a nonlinear function of the stress tensor. We consider a special case of (9), where we assume there exists a scalar function  $\Pi = \Pi(\mathbf{T})$  such that (see Ref. [16])

$$\boldsymbol{\varepsilon} = \mathbf{g}(\mathbf{T}) = \frac{\partial \Pi}{\partial \mathbf{T}}. \quad (10)$$

If  $\Pi$  is assumed to be an isotropic function, we have that  $\Pi(\mathbf{T}) = \Pi(J_1, J_2, J_3)$ , where  $J_i = 1, 2, 3$  are the following set of invariants of the stress tensor

$$J_1 = \text{tr} \mathbf{T}, \quad J_2 = \frac{1}{2} \text{tr}(\mathbf{T}^2), \quad J_3 = \frac{1}{3} \text{tr}(\mathbf{T}^3). \quad (10)$$

And from (10), we obtain the representation

$$\boldsymbol{\varepsilon} = \Pi_1 \mathbf{I} + \Pi_2 \mathbf{T} + \Pi_3 \mathbf{T}^2, \quad (12)$$

Where  $\Pi_i = \frac{\partial \Pi}{\partial J_i}$ ,  $i = 1, 2, 3$ .

The following particular expression for  $\Pi$  is considered:

$$\Pi(J_1, J_2) = -\frac{\alpha}{\beta} \ln[\cosh(\beta J_1)] + \frac{\gamma}{\iota} \sqrt{1 + 2\iota J_2}, \quad (13)$$

Where  $\alpha, \beta, \gamma$  and  $\iota$  are constants.

Eq. (13) has been used in Ref. [17] to study problems, where independently of the magnitude of the stresses, the strains remains small. It is necessary to point out that this form for  $\Pi$  and the numerical values of the constant that are shown in Table 1, have not been obtained from experimental data. In Figures 1, 2 presented in Ref. [17], some plots for the behavior of a cylinder under tension are shown, where it is possible to observe that the strains remain always small independently of the magnitude of the stresses. As indicated in the introduction section, such particular expressions could be important for fracture analysis of brittle bodies. Finally, in Table 1 the numerical values of the constants used in (6) and (13) are presented.

$\alpha$	$\beta$ 1/Pa	$\gamma$ 1/Pa	$\iota$ 1/Pa <sup>2</sup>	$\mu$ Pa	$\kappa$ Pa
0.01	$9.277 \times 10^{-8}$	$4.020 \times 10^{-9}$	$10^{-14}$	$80.194 \times 10^6$	$150 \times 10^6$

**Table 1.** Values for the constants used in (6) and (13).

### 2.3. Boundary value problems

For the hyper-elastic cylinder, the boundary value problem is the classical formulation in nonlinear elasticity, where the function  $\chi(X)$  is found by solving the equilibrium equation in the reference configuration (see, for example, Ref. [4]):

$$\text{Div} \mathbf{S} = \mathbf{0}, \quad (14)$$

Where  $\mathbf{S} = J^{-1} \mathbf{F} \mathbf{T}$  is the nominal stress tensor. From (5),  $s = \frac{\partial W}{\partial \mathbf{F}}$ , and Div is the divergence operator with respect to the reference configuration. Eq. (14) must be solved using the boundary conditions

$$\mathbf{S}^T \mathbf{N} = \hat{\mathbf{s}} \quad \mathbf{X} \in \partial \mathcal{B}_r^s, \quad \chi = \hat{\mathbf{x}} \quad \mathbf{X} \in \partial \mathcal{B}_r^x, \quad (15)$$

Where  $\partial \mathcal{B}_r$  is the boundary of the hyper-elastic body in the reference configuration,  $\partial \mathcal{B}_r^s \cup \partial \mathcal{B}_r^x = \partial \mathcal{B}_r$ ,  $\partial \mathcal{B}_r^s \cap \partial \mathcal{B}_r^x = \emptyset$ ,  $\mathbf{N}$  is the outward normal vector to the surface of the body in the reference configuration,  $\mathbf{s}$  is the external traction (described in the reference configuration), and  $\mathbf{x}$  is a known deformation field on some part of the surface of the hyper-elastic body.

For the inclusions we consider small strains and displacements. And following what has been presented in Refs. [16, 17], for the boundary value problem corresponds to find  $\mathbf{T}$  and  $\mathbf{u}$  by solving (see (3), (4) and (10))

$$\text{div} \mathbf{T} = \mathbf{0}, \quad \frac{1}{2} (\nabla \mathbf{u} + \nabla \mathbf{u}^T) = \frac{\partial \Pi}{\partial \mathbf{T}} \quad (16)$$

simultaneously. In the above system we have 9 equations for a fully 3D problem, and 9 unknowns that correspond to the components of the stress tensor and the displacement field. Regarding the boundary conditions we have in general

$$\mathbf{T} \mathbf{n} = \hat{\mathbf{t}} \quad \mathbf{x} \in \partial \mathcal{B}_t^t, \quad \mathbf{u} = \hat{\mathbf{u}} \quad \mathbf{x} \in \partial \mathcal{B}_t^u, \quad (17)$$

Where  $\partial \mathcal{B}_t$  is the surface of the inclusion and  $\mathbf{x} \in \partial \mathcal{B}_t^t \cup \partial \mathcal{B}_t^u = \partial \mathcal{B}_t$ ,  $\partial \mathcal{B}_t^t \cap \partial \mathcal{B}_t^u = \emptyset$ ,  $\mathbf{n}$  is the normal vector to the surface of the inclusion,  $\mathbf{t}$  is the external load and  $\mathbf{u}$  is a known displacement field on a part of the surface of the

inclusion. Since for the inclusion we assumed that  $|\nabla u| \sim O(\delta)$  where  $\delta \ll 1$ , then there is no need for distinguishing between the reference and the current configuration for that body.

### 3. AXIAL-SYMMETRIC MODELS

For simplicity, the hyper-elastic matrix is considered to be a cylinder of radius  $R$  and length  $L$  (see, for example, Figure 1). For a cylinder with one inclusion, it is assumed that the inclusion is located in the center of the cylinder, and that the radius of that spherical body is  $r_i$  (see Figure 1). It is assumed that there is axial symmetry, therefore, we study a plane problem using the coordinates  $r$  and  $z$  (radial and axial axis, respectively).

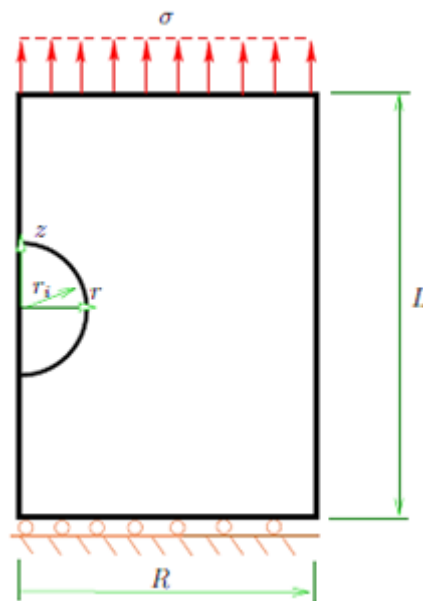
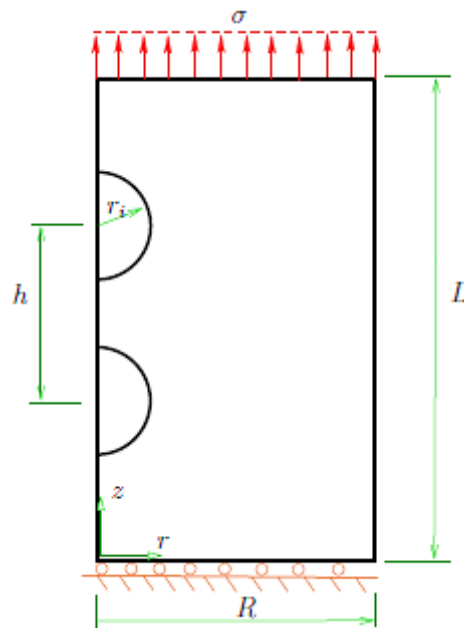


Figure 1. Hyper-elastic cylinder with one inclusion.

The center of the sphere is located at  $z = L/2$ . On the surface  $z = L$  we apply a uniform axial load  $\sigma$ . On the surface  $z = 0$  we assume that the cylinder cannot move in the axial direction, but it is free to expand in the radial direction, i.e.,  $u_z(r, 0) = 0$ . On the surface  $r = R$  we assume that the cylinder is free. Finally, the spherical inclusion is assumed to be perfectly bonded to the surrounding hyper-elastic cylinder, i.e., the displacement field is continuous across the surface of the inclusion.

In Figure 2, an hyper-elastic cylinder with two inclusions is depicted.



**Figure 2.** Hyper-elastic cylinder with two inclusions.

These two inclusions are of the same radius, are separated by a distance  $h$  between centers (the central point between them is located in the middle of the cylinder in the axial line defining it.) The two inclusions are assumed to behave as nonlinear elastic bodies using (10). The rest of the boundary conditions for the problem are the same as the problem presented in Figure 1.

In Figure 3, the case of an hyper-elastic cylinder with five inclusions in a row is presented.



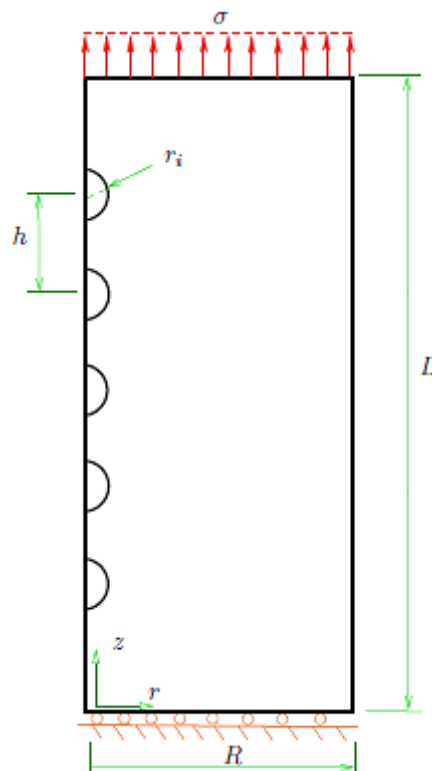


**Figure 3.** Hyper-elastic cylinder with five inclusions.

The inclusions are separated to each other by the same distance  $h$ . As in the previous case, they are modelled using (10), and the center point for all the inclusions is located in the center of the cylinder.

For the different models mentioned previously, it was assumed that  $r_i = 1$  mm. Regarding  $R$ ,  $L$  and  $h$ , different cases were considered as indicated in Tables 2-4.

$R$	$2r_i$	$3r_i$	$4r_i$	$5r_i$
$L$	$6r_i$	$8r_i$	$10r_i$	

**Chart 2.** Cases studied for the cylinder with one inclusion.

For the case of a cylinder with two inclusions, we assume  $R = 5r_i$  and  $L = 10r_i$  (the parameter  $h$  is presented in Chart 3.)

$h$	$2.1r_i$	$2.2r_i$	$2.3r_i$	$2.4r_i$	$2.5r_i$	$3r_i$	$4r_i$	$5r_i$
-----	----------	----------	----------	----------	----------	--------	--------	--------

**Chart 3.** Cases studied for the cylinder with two inclusions.

Finally, for the case of a cylinder with five inclusions, we assume  $R = 5r_i$  and  $L = 4(h + r_i)$ , and for  $h$  we have the cases presented in Chart 4.

$h$	$2.1r_i$	$2.2r_i$	$2.3r_i$	$2.4r_i$	$2.5r_i$	$3r_i$	$4r_i$	$5r_i$	$6r_i$	$7r_i$
-----	----------	----------	----------	----------	----------	--------	--------	--------	--------	--------

**Chart 4.** Cases studied for the cylinder with five inclusions.

The boundary value problems were solved using the finite element method with an in-house finite element code (details of the method in which the code is based can be found, for example, in Ref. [16].)

## 4. NUMERICAL RESULTS

### 4.1. Results for one inclusion

In this section we show some results for a cylinder with one spherical inclusion located on its center (see Figure 1), for the cases indicated in Table 2.

In Figure 4, results are presented for the axial and radial components of the normalized stress and the components of the strain, for different values for  $R$ , for the case  $L = 10 r_i$ .

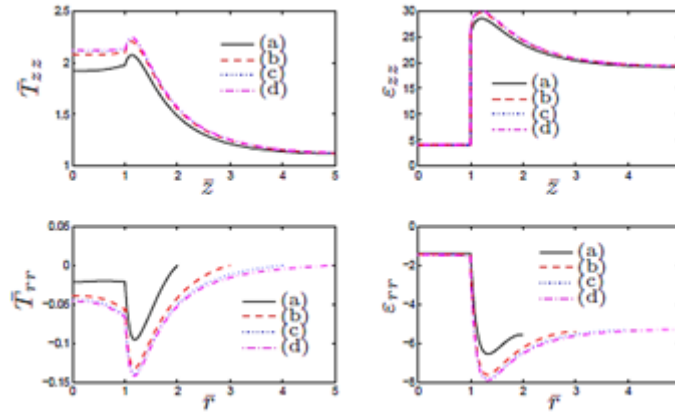


**Figure 4.** Results for the normalized components of the stress  $T_{zz}$  and strain  $\epsilon_{zz}$ , for the line  $r = 0, 0 \leq z \leq L/2$ , and the component  $T_{rr}$  of the stress and  $\epsilon_{rr}$  of the strain, for the line  $z = 0, 0 \leq r \leq R$ . This is for the case  $L = 10 r_i$ , where: (a)  $R = 2 r_i$  (b)  $R = 3 r_i$  (c)  $R = 4 r_i$  (d)  $R = 5 r_i$ .

The normalized components of the stress that appear in Figure 4 are defined as.

$$\bar{T}_{zz} = \frac{T_{zz}}{\sigma}, \quad \bar{T}_{rr} = \frac{T_{rr}}{\sigma}, \quad (18)$$

Where  $\sigma$  is the uniform load applied on the upper surface of the cylinder (see Figure 1). The strains are in %. The results for the axial components of the normalized stress and strain  $T_{zz}$  and  $\epsilon_{zz}$  presented in Figure 4, respectively, are shown for the line  $r = 0, 0 \leq \bar{z} \leq \bar{L}/2$ , where

$$\bar{z} = \frac{z}{r_i}, \quad \bar{L} = \frac{L}{r_i}. \quad (19)$$

The results for the radial components of the normalized stress and strain  $\bar{T}_{rr}$  and  $\epsilon_{rr}$ , presented in Figure 4, respectively, are shown for the line  $z = 0, 0 \leq \bar{r} \leq \bar{R}$ , where.

$$\bar{r} = \frac{r}{r_i}, \quad \bar{R} = \frac{R}{r_i}. \quad (20)$$

In Figure 5 we show similar results as in Figure 4, for  $R = 5 r_i$  and different cases for  $L$ .

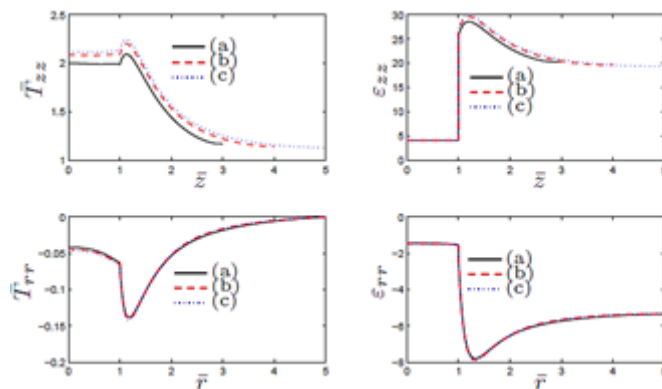


**Figure 5.** Results for the normalized components of the stress  $T_{zz}$  and strain  $\epsilon_{zz}$ , for the line, and the component  $T_{rr}$  of the stress and  $\epsilon_{rr}$  of the strain, for the line  $z = 0$ ,  $0 \leq r \leq R$ . This is for the case  $R = 5 r_i$ , where (a)  $L = 6 r_i$  (b)  $L = 8 r_i$  (c)  $L = 10 r_i$ .

The results for  $T_{zz}$  and  $\epsilon_{zz}$  are shown for the line  $r = 0$ ,  $0 \leq z \leq \bar{L}$ , while for  $T_{rr}$  and  $\epsilon_{rr}$ , the results are shown for the line  $z = 0$ ,  $0 \leq \bar{r} \leq R$ .

In both Figures 4 and 5 the inclusion is located in the region  $\bar{r} \leq 1$ ,  $\bar{z} \leq 1$ , and due to the symmetry of the problem, only the upper half part of the inclusion and the cylinder is considered (see Figure 1).

In Figures 6-9 we show results for the radial and axial components of the strain and the stress, for the case  $R = 5 r_i$ ,  $L = 10 r_i$ . The stresses are presented in Pa.

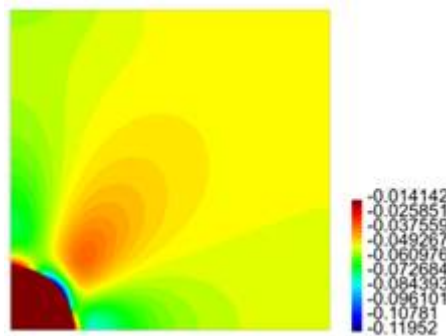


**Figure 6.** Contour plot for  $\epsilon_{rr}$  for the problem of one inclusion.

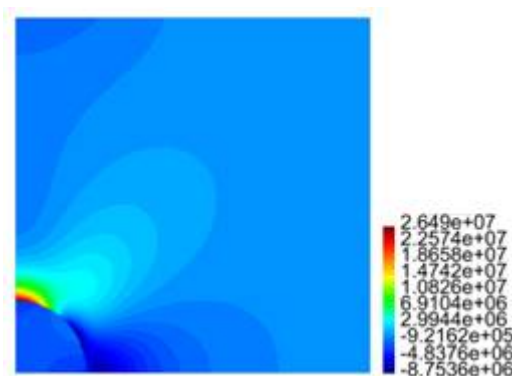


**Figure 7.** Contour plot for  $T_{rr}$  in Pa for the problem of one inclusion.

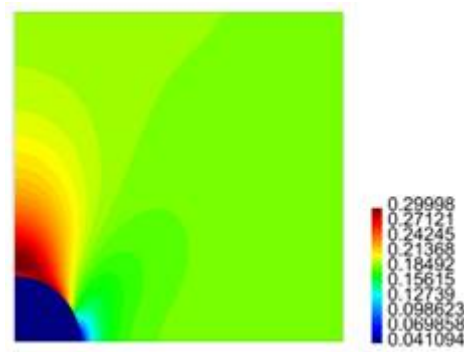


Figure 8. Contour plot for  $T_{rr}$  for the problem of one inclusion.

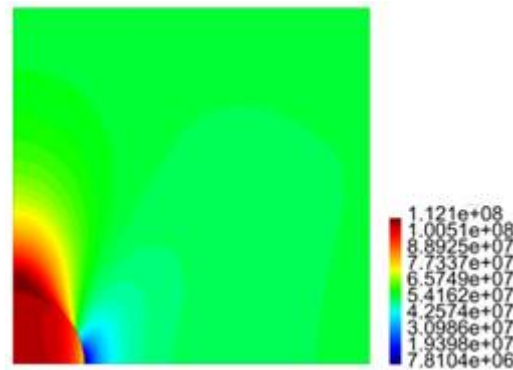


Figure 9. Contour plot for  $T_{zz}$  in Pa for the problem of one inclusion.

## 4.2. Results for two inclusions

Figure 10 depicts results for the axial and radial components of the stress (normalized stresses, see (18)) and the strain, for the line  $r = 0$ ,  $0 \leq z \leq L$ , for different values for  $h$  as presented in Chart 3 for a hyperelastic cylinder with two inclusions (see Figure 2).

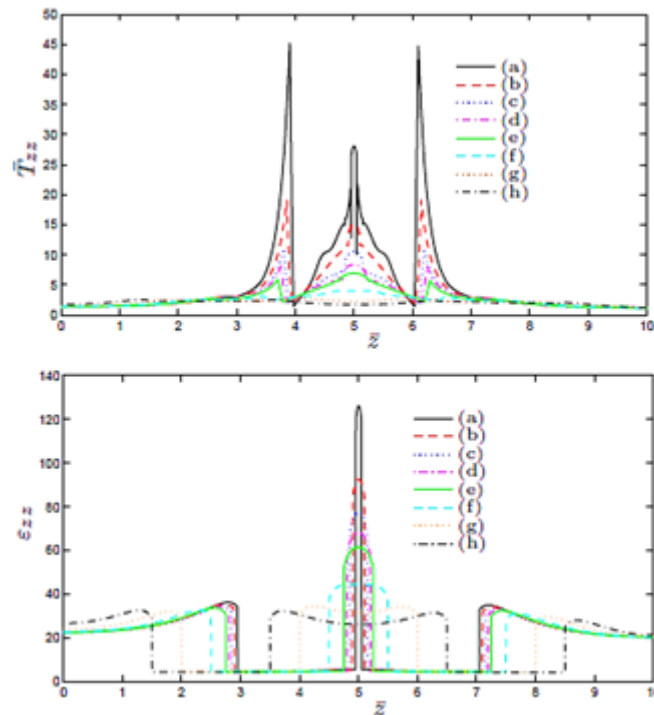


Figure 10. Results for the normalized components of the stress  $T_{zz}$  and strain  $\epsilon_{zz}$ , for the line  $r = 0$ ,  $0 \leq z \leq L$ , where (a)  $h = 2.1$  ri (b)  $h = 2.2$  ri (c)  $h = 2.3$  ri (d)  $h = 2.4$  ri (e)  $h = 2.5$  ri (f)  $h = 3$  ri (g)  $h = 4$  ri (h)  $h = 5$  ri.

In Figures 11-14 we present results for the radial and axial components of the strain and the stress, for the case  $h = 2.5$  (the stresses are in Pa.)

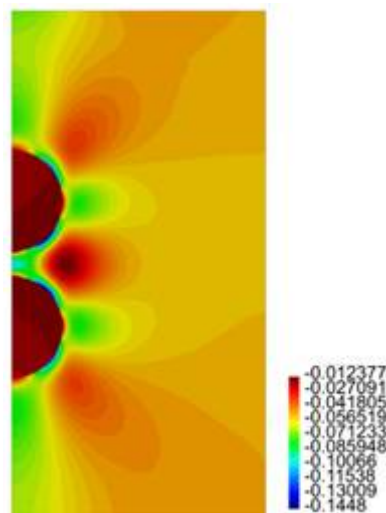


Figure 11. Contour plot for  $\epsilon_{rr}$  for the problem of two inclusions.

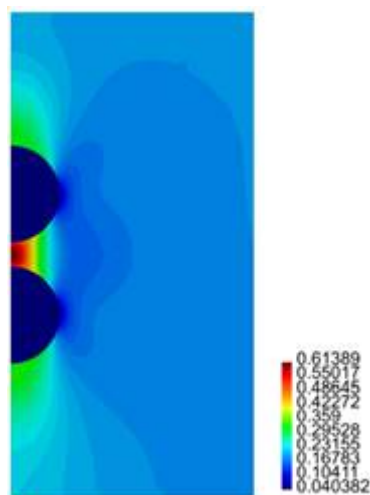


Figure 12. Contour plot for  $T_{rr}$  in Pa for the problem of two inclusions.

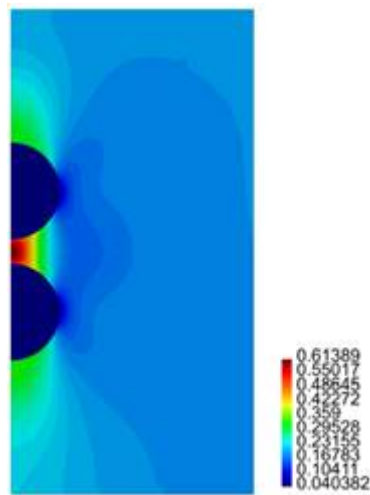


Figure 13. Contour plot for  $\epsilon_{zz}$  for the problem of two inclusions.

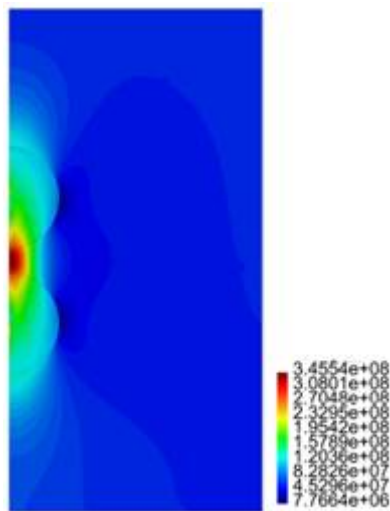
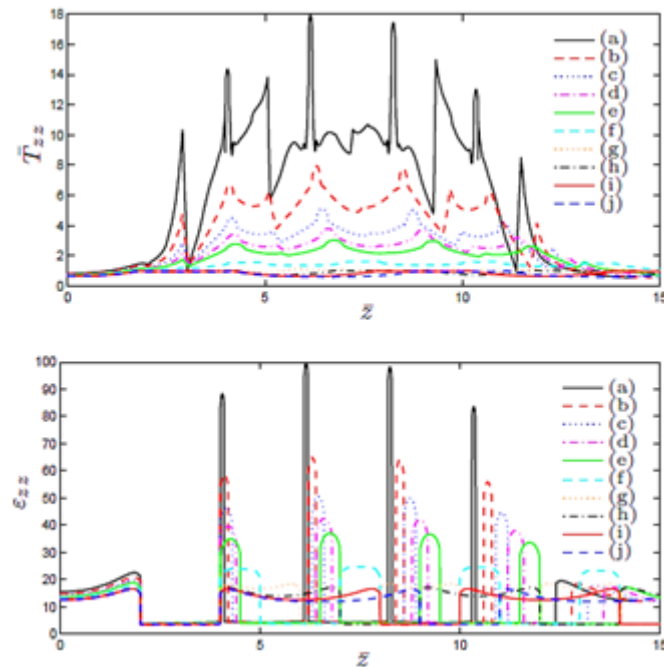


Figure 14. Contour plot for  $T_{zz}$  in Pa for the problem of two inclusions.

### 4.3. Results for five inclusions

Figure 15 presents results for the axial and radial components of the stress (normalized stresses, see (18)) and the strain, for the line  $r = 0$ ,  $0 \leq \bar{z} \leq \bar{L}$  for a hyperelastic cylinder with five inclusions (see Figure 3).



**Figure 15.** Results for the normalized components of the stress  $T_{zz}$  and strain  $\epsilon_{zz}$ , for the line  $r = 0$ ,  $0 \leq z \leq L$ , where (a)  $h = 2.1 r_i$  (b)  $h = 2.2 r_i$  (c)  $h = 2.3 r_i$  (d)  $h = 2.4 r_i$  (e)  $h = 2.5 r_i$  (f)  $h = 3 r_i$  (g)  $h = 4 r_i$  (h)  $h = 5 r_i$  (i)  $h = 6 r_i$  (j)  $h = 7 r_i$ .

In Figures 16-19 we present results for the radial and axial components of the strain and the stress, for the case  $h = 2.5 r_i$  (the stresses are in Pa.)

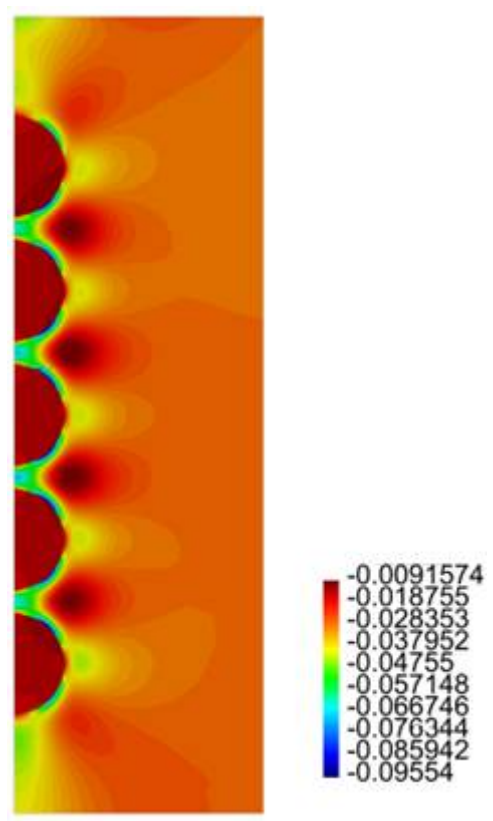


Figure 16. Contour plot for  $\epsilon_{rr}$  for the problem of five inclusions.

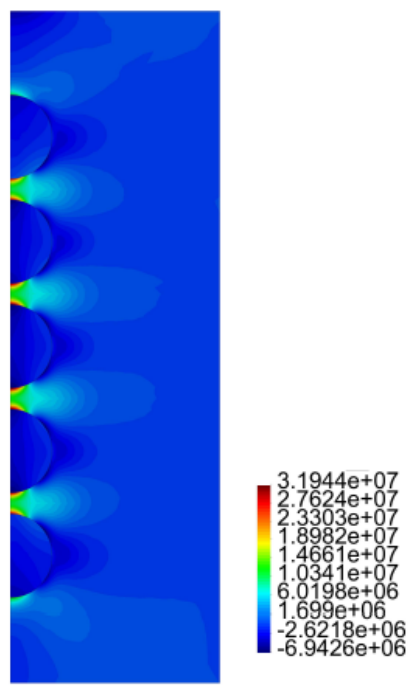


Figure 17. Contour plot for  $T_{rr}$  in Pa for the problem of five inclusions



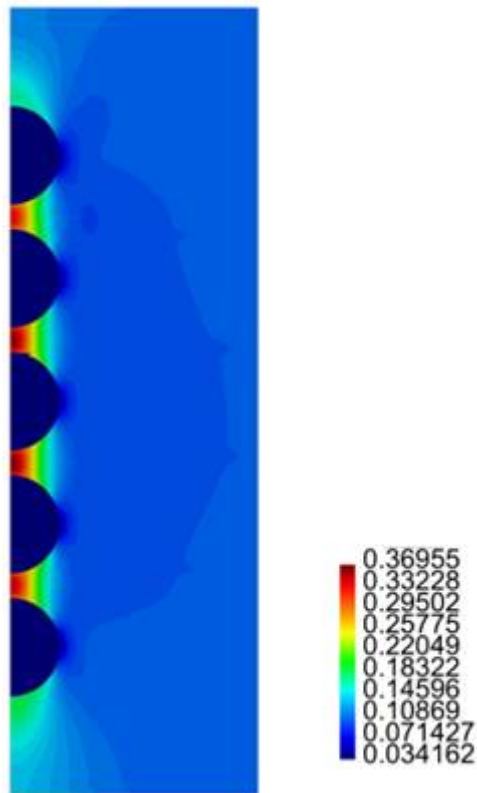


Figure 18. Contour plot for  $\epsilon_{zz}$  for the problem of five inclusions.

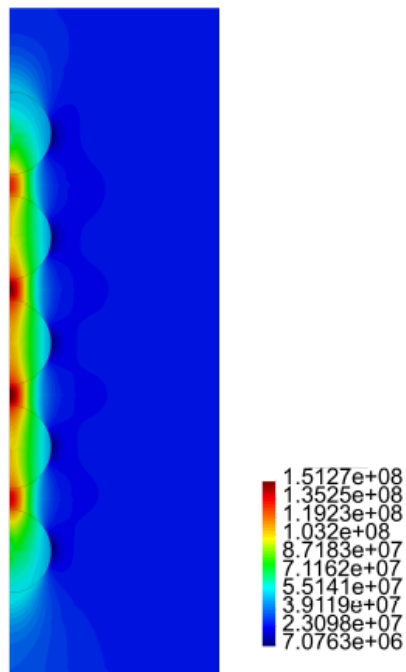


Figure 19. Contour plot for  $T_{zz}$  in Pa for the problem of five inclusions.

#### 4.4. Discussion of the results

For the matrix with one particle, from Figure 4 cases c) and (d), it is observed there is no meaningful difference between the behaviour of the stress and the strain, i.e., as expected for  $R$  large enough, the results tend to be invariant of the size of the cylinder. For the results presented in Figure 5, as in the previous case, for  $L$  large enough, there is no much difference in the behaviour of the body. From Figures 4 and 5, we observe that the component of the stress are continuous across the surface of the inclusion, but the components of the strain are not. In both cases, it is recognized the presence of large stresses in the matrix material near the interface with the inclusion, and for  $T_{zz}$  such stresses are positive, which could eventually lead to debonding of the composite. In fact, in Figure 7 we recognize that there is a zone on the upper part of the spherical inclusion (in the matrix), where the radial stress  $T_{rr}$  is positive, and that effect is much stronger in the same zone for  $T_{zz}$  (see Figure 9).

For the cylinder with two spherical inclusions, from Figure 10 we observe that there is a considerable difference in the behaviour of the composite if  $h$  is varied. Compare for instance the results presented in cases (a), (b) and (d) of that figure, where  $h = 2.1 r_i$ ,  $h = 2.2 r_i$  and  $h = 2.3 r_i$ , respectively. The difference in behaviour between  $T_{zz}$  and  $\epsilon_{zz}$  is large (in particular for the case (a) for  $T_{zz}$ .) In the plot for  $\epsilon_{zz}$ , we observe the jump in the value for that component of the strain across the interface between the inclusion and the surrounding matrix. In Figures 12, 14 we notice the large values for  $T_{rr}$  and  $T_{zz}$  in the matrix, for the zone connecting the two inclusions.

Finally, for the cylinder with five inclusions, as in the previous case, from Figure 15 we notice large values for  $\epsilon_{zz}$  for the matrix material between the inclusions. Also large values and rapid variations for  $T_{zz}$  in the same zone are observed, especially for the cases (a), (b) and (c). From Figures 16-19 we observe the same large values for the components of the stress and the strain in the zone near the inclusions.

#### 5. CONCLUDING REMARKS

In the present communication, we have studied the behaviour of a composite consisting of a hyper-elastic matrix with one, two and five spherical inclusions that are modelled using some relatively new classes of constitutive equations, in which, as a particular case such inclusions undergo small strains independently of the magnitude of the stresses. In several of the previous works discussed in the introduction section (see, for example, Refs. [10, 17] and the reference mentioned therein), the main idea of studying constitutive equations of the type (10), (13), was to analyse the behaviour of the solutions for problems exhibiting concentration of stresses, where from the physical point of view, it is expected that the strain remain small. This is the case of brittle bodies with cracks (see the discussion in Ref. [14]). In the present work, this has been also the purpose. Herein, problems exhibiting concentration of stresses near the boundary of inclusions were studied. From the results presented in Section 4, it is observed that indeed there exists concentration of stresses, but strains remain small inside the inclusions. The results presented in this paper should be considered as the outcome of a new way to study the problem of modelling the behaviour of composite materials, where there is a soft matrix filled with a relatively stiff and brittle inclusions.

#### ACKNOWLEDGMENT

The authors would like to express his gratitude for the financial support provided by FONDECYT (Chile) under grant no. 1120011. The work of S. Montero was also funded by a Scholarship for master degree students provided by CONICYT (Chile).

## REFERENCES

- [1] K. R. Rajagopal, "On implicit constitutive theories," *Applications of Mathematics*, vol. 48, no. 4, pp. 279–319, 2003, advances in Material & Processing Technologies Conference. [Online]. Available: <https://doi.org/10.1023/A:1026062615145>
- [2] —, "The elasticity of elasticity," *Zeitschrift für angewandte Mathematik und Physik*, vol. 58, no. 2, pp. 309–317, 2007, advances in Material & Processing Technologies Conference. [Online]. Available: <https://doi.org/10.1007/s00033-006-6084-5>
- [3] K. Rajagopal and A. Srinivasa, "On the response of non-dissipative solids," *Proceedings of the Royal Society of London A: Mathematical, Physical and Engineering Sciences*, vol. 463, no. 2078, pp. 357–367, 2007. [Online]. Available: <https://dx.doi.org/10.1098/rspa.2006.1760>
- [4] N. W. Truesdell, C., *The non-linear field theories of mechanics*, 3rd ed., S. Antman, Ed. Springer Berlin Heidelberg, 2004. [Online]. Available: <https://doi.org/10.1007/s00170-011-3267-9>
- [5] K. R. Rajagopal and U. Saravanan, "Extension, inflation and circumferential shearing of an annular cylinder for a class of compressible elastic bodies," *Mathematics and Mechanics of Solids*, vol. 17, no. 5, pp. 473–499, 2012. [Online]. Available: <https://doi.org/10.1177/1081286511423125>
- [6] R. Bustamante and K. R. Rajagopal, "A nonlinear model for describing the mechanical behaviour of rock," *Acta Mechanica*, pp. 1–22, 2017. [Online]. Available: <https://doi.org/10.1007/s00707-017-1968-3>
- [7] P. A. Johnson and P. N. J. Rasolofosaon, "Manifestation of nonlinear elasticity in rock: Convincing evidence over large frequency and strain intervals from laboratory studies," *Nonlinear Processes in Geophysics*, vol. 3, no. 2, pp. 77–88, 1996. [Online]. Available: <https://goo.gl/bnyjUK>
- [8] Z. Grasley, R. El-Helou, M. D'Ambrosia, D. Mokarem, C. Moen, and K. Rajagopal, "Model of infinitesimal nonlinear elastic response of concrete subjected to uniaxial compression," *Journal of Engineering Mechanics*, vol. 141, no. 7, p. 04015008, 2015. [Online]. Available: [https://dx.doi.org/10.1061/\(ASCE\)EM.1943-7889.0000938](https://dx.doi.org/10.1061/(ASCE)EM.1943-7889.0000938)
- [9] V. Kulvait, J. Málek, and K. R. Rajagopal, "Modeling gum metal and other newly developed titanium alloys within a new class of constitutive relations for elastic bodies," *Archives of Mechanics*, vol. 69, no. 3, pp. 223–241, 2017. [Online]. Available: <https://goo.gl/qLkpQP>
- [10] —, "Anti-plane stress state of a plate with a v-notch for a new class of elastic solids," *International Journal of Fracture*, vol. 179, no. 1–2, pp. 59–73, 2013. [Online]. Available: <https://doi.org/10.1007/s10704-012-9772-5>
- [11] M. L. Williams, "On the stress distribution at the base of a stationary crack," *Journal of Applied Mechanics*, vol. 24, no. 1, pp. 10\*–114, 1956. [Online]. Available: <https://goo.gl/q9uZUn>
- [12] H. Zhu, A. Muliana, and K. Rajagopal, "On the nonlinear viscoelastic deformations of composites with prestressed inclusions," *Composite Structures*, vol. 149, Supplement C, pp. 279–291, 2016. [Online]. Available: <https://doi.org/10.1016/j.compstruct.2016.03.008>
- [13] C. Truesdell and R. Toupin, *The classical field theories*. Springer, Berlin, Heidelberg: *Principles of Classical Mechanics and Field Theory / Prinzipien der Klassischen Mechanik und Feldtheorie*. *Encyclopedia of Physics / Handbuch der Physik*, 1960, vol. 2/3/1, pp. 226–858. [Online]. Available: [https://doi.org/10.1007/978-3-642-45943-6\\_2](https://doi.org/10.1007/978-3-642-45943-6_2)
- [14] K. R. Rajagopal, "On the nonlinear elastic response of bodies in the small strain range," *Acta Mechanica*, vol. 225, no. 6, pp. 1545–1553, 2014. [Online]. Available: <https://doi.org/10.1007/s00707-013-1015-y>
- [15] R. Bustamante and K. R. Rajagopal, "A note on plane strain and plane stress problems for a new class of elastic bodies," *Mathematics and Mechanics of Solids*, vol. 15, no. 2, pp. 229–238, 2010. [Online]. Available: <https://doi.org/10.1177/1081286508098178>
- [16] A. Ortiz-Bernardin, R. Bustamante, and K. Rajagopal, "A numerical study of elastic bodies that are described by constitutive equations that exhibit limited strains," *International Journal of Solids and Structures*, vol. 51, no. 3, pp. 875–885, 2014. [Online]. Available: <https://doi.org/10.1016/j.ijsolstr.2013.11.014>

- [17] S. Montero, R. Bustamante, and A. Ortiz- Bernardin, “A finite element analysis of some boundary value problems for a new type of constitutive relation for elastic bodies,” *Acta Mechanica*, vol. 227, no. 2, pp. 601–615, 2016. [Online]. Available: <https://doi.org/10.1007/s00707-015-1480-6>